

Ultraviolet Electroluminescence from MgZnO-Based Heterojunction Light-Emitting Diodes

H. Zhu,^{†,‡} C. X. Shan,^{*,†} B. H. Li,[†] J. Y. Zhang,[†] B. Yao,[†] Z. Z. Zhang,[†] D. X. Zhao,[†] D. Z. Shen,[†] and X. W. Fan[†]

Key Laboratory of Excited State Processes, Changchun Institute of Optics, Fine Mechanics and Physics, Chinese Academy of Sciences, Changchun 130033, China, and Graduate School of Chinese Academy of Sciences, Beijing 100049, China

Received: November 10, 2008; Revised Manuscript Received: December 22, 2008

We report on the fabrication of an $n\text{-Mg}_{0.12}\text{Zn}_{0.88}\text{O}/p\text{-GaN}$ heterojunction light-emitting diode with an MgO dielectric interlayer by plasma-assisted molecular beam epitaxy. The current–voltage curve of the heterojunction diode showed obvious rectifying characteristics with a threshold voltage of about 8 V. Under forward bias, an ultraviolet electroluminescence (EL) emission located at about 374 nm coming from the $\text{Mg}_{0.12}\text{Zn}_{0.88}\text{O}$ layer was observed at room temperature. This is one of the shortest EL emissions observed in ZnO-based pn junctions to the best of our knowledge. The origin of the EL emission was elucidated in terms of the carrier transportation process modulated by the MgO interlayer in the heterojunction.

Introduction

Short-wavelength semiconductor light-emitting devices and laser diodes have attracted much attention for their versatile applications in data storage, lighting, displays, etc. Zinc oxide (ZnO) has been considered one of the strongest candidate materials for such applications because of its wide band gap and large exciton binding energy. However, the main hurdle that hinders the applications of ZnO is the huge difficulty in obtaining high-quality p -type ZnO.¹ A natural route to avoiding this hurdle is to employ other available p -type materials such as NiO,² GaN,^{3–6} AlGaIn,⁷ SiC,⁸ or SrCu_2O_2 ⁹ to form pn junctions with $n\text{-ZnO}$. Among these materials, GaN is highlighted because it has the same wurtzite structure as ZnO, and the in-plane lattice mismatch between these two materials is very small (1.8%), which promises high-quality heterojunctions are attainable in a ZnO–GaN system. However, in many cases, the ZnO–GaN heterojunction diode shows a strong electroluminescence (EL) emission at about 430 nm,^{3,10} which comes from the donor–acceptor pair recombination in Mg-doped $p\text{-GaIn}$, while the emission from ZnO is weak. This is because the hole concentration and mobility in GaN are usually lower than the corresponding values of electrons in ZnO. As a result, holes in GaN do not diffuse into ZnO, instead electrons in ZnO enter into GaN. In that case, the merits of ZnO have not been fully exploited. In our previous publication, a thin MgO layer was employed to confine electrons in the ZnO layer, while holes can tunnel through the MgO layer and enter into ZnO from $p\text{-GaIn}$. Consequently, the EL emission from ZnO was greatly enhanced, and an intense emission at about 400 nm (3.1 eV) originating from ZnO has been obtained in our case.¹¹ Realizing EL with a shorter wavelength is of great significance in a variety of fields, including air and water purification, food disinfection, and biomedical instrumentation, etc., and its study is a main goal of researchers. It is rational to speculate that by replacing ZnO in our aforementioned ZnO–MgO–GaN heterojunction with materials having a larger band gap, we can attain EL

emissions with shorter wavelengths. Ohtomo et al. have demonstrated that the band gap of ZnO can be widened up to 4.0 eV without phase separation by incorporating Mg into the ZnO lattice.¹² From then on, high-quality $\text{Mg}_x\text{Zn}_{1-x}\text{O}$ alloys have been grown with a variety of deposition techniques such as pulsed laser deposition,^{12,13} molecular beam epitaxy,^{14–16} metal–organic vapor phase epitaxy,¹⁷ etc. However, there is only one report on EL emissions from a $\text{MgZnO } pn$ homojunction that has been found to the best of knowledge.¹⁸ This is due to the fact that p -type doping of ZnO is still a challenge, as is p -type doping of MgZnO with a larger band gap. Therefore, it is a natural choice to combine $n\text{-MgZnO}$ and $p\text{-GaIn}$ together to form a pn heterojunction. However, no report on such a heterojunction has been found to the best of our knowledge.

In this paper, $n\text{-MgZnO}$ film has been deposited onto $p\text{-GaIn}$ to form a pn junction. By proper engineering of the band alignment of the heterojunction using a dielectric MgO interlayer, most electrons are confined in the MgZnO layer, while holes can be injected into the MgZnO layer from the $p\text{-GaIn}$ layer. In this way, EL emission at around 374 nm coming from the MgZnO layer has been obtained. The mechanism for the EL has been discussed in terms of the carrier transportation process in the heterojunction.

Experimental Section

The heterojunction was prepared by depositing $\text{Mg}_x\text{Zn}_{1-x}\text{O}$ film (500 nm in thickness) onto a commercially available $p\text{-GaIn}/\text{Al}_2\text{O}_3$ template using a plasma-assisted molecular beam epitaxy (MBE) technique, and a 20 nm MgO dielectric layer was also grown as an interlayer between the MgZnO and GaN layer. The role of the MgO layer was to reduce the interface defects as well as modulate the carrier transportation in the heterojunction, which has been detailed in our previous publication.¹¹ The $p\text{-GaIn}$ layer was 2 μm in thickness, and the hole concentration and mobility were $3 \times 10^{17} \text{ cm}^{-3}$ and $10 \text{ cm}^2 \text{ V}^{-1} \text{ s}^{-1}$, respectively. Precursors used for the growth of MgO and MgZnO were elemental zinc (6 N in purity), elemental magnesium (6 N in purity), and O_2 gas (5 N in purity). The O_2 gas was activated by an Oxford Applied Research radio frequency plasma cell (model HD25) operating at 13.56 MHz.

* To whom correspondence should be addressed. E-mail: phycxshan@yahoo.com.cn.

[†] Changchun Institute of Optics, Fine Mechanics and Physics.

[‡] Graduate School of Chinese Academy of Sciences.

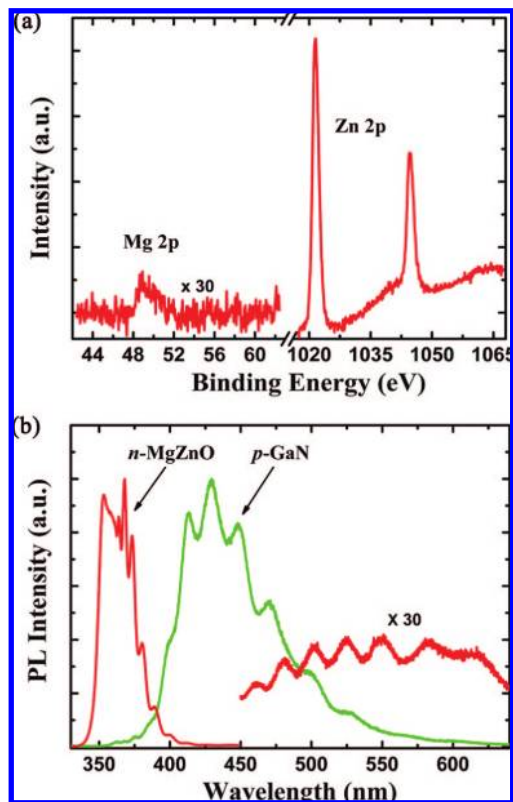


Figure 1. (a) XPS spectrum of the $\text{Mg}_x\text{Zn}_{1-x}\text{O}$ layer; note that the Mg signal has been magnified 30 times for clarity. (b) Normalized room-temperature PL spectra of the $n\text{-Mg}_{0.12}\text{Zn}_{0.88}\text{O}$ and $p\text{-GaN}$ layers; the deep-level emission of MgZnO was magnified 30 times for comparison.

The substrate temperature was fixed at 700 °C, the chamber pressure at 2×10^{-6} mbar, and the oxygen flow rate at 1.25 sccm during the growth process. The as-grown MgZnO film showed n -type conduction with an electron concentration of $9 \times 10^{16} \text{ cm}^{-3}$ and a mobility of $2 \text{ cm}^2 \text{ V}^{-1} \text{ S}^{-1}$. The Mg content of the $\text{Mg}_x\text{Zn}_{1-x}\text{O}$ film was determined by X-ray photoelectron spectroscopy (XPS). Photoluminescence (PL) measurement was carried out with a JY-630 micro-Raman spectrometer employing the 325 nm line of a He–Cd laser as the excitation source. Ohmic contacts were achieved by vacuum evaporating In and Ni–Au layers onto the $n\text{-Mg}_x\text{Zn}_{1-x}\text{O}$ and $p\text{-GaN}$ layers, respectively, and the electrical properties of the films were measured with a Hall measurement system (LakeShore 7707). EL spectra of the heterojunction diode were recorded at room temperature in an F4500 spectrometer, and a continuous current power source was used to excite the heterojunction diode.

Results and Discussion

Figure 1a shows the XPS spectrum of the $\text{Mg}_x\text{Zn}_{1-x}\text{O}$ layer. The intensity of Mg 2p has been magnified 30 times for comparison. Mg content x in the $\text{Mg}_x\text{Zn}_{1-x}\text{O}$ film was determined to be 0.12 from the XPS spectrum. Shown in Figure 1b are the room-temperature PL spectra of the $n\text{-Mg}_{0.12}\text{Zn}_{0.88}\text{O}$ and $p\text{-GaN}$ layers. The spectrum of the $\text{Mg}_{0.12}\text{Zn}_{0.88}\text{O}$ layer shows an intense emission at 356 nm and some sharp fringes at around 368 nm. We note the peak at 356 nm comes from the near band edge (NBE) emission of $\text{Mg}_{0.12}\text{Zn}_{0.88}\text{O}$, while the fringes centered at 368 nm come from the interference between the upper and lower interfaces of the MgZnO film. The appearance of such interference peaks reveals that the film is very smooth. Additionally, there appears to be a weak broad emission located

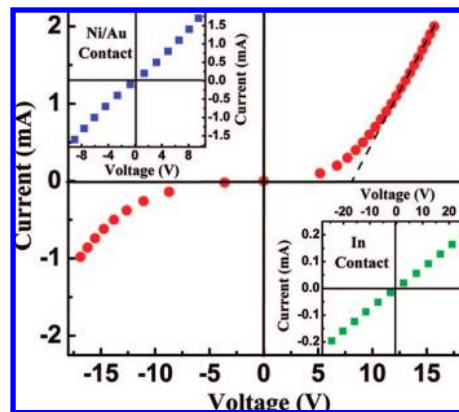


Figure 2. I – V curve of the $n\text{-Mg}_{0.12}\text{Zn}_{0.88}\text{O}$ – MgO – $p\text{-GaN}$ heterojunction diode. The dashed line is a guide for the eyes. The inset illustrates the I – V curve of the Ni–Au contact with the $p\text{-GaN}$ and the In contact with the $n\text{-Mg}_{0.12}\text{Zn}_{0.88}\text{O}$ layers.

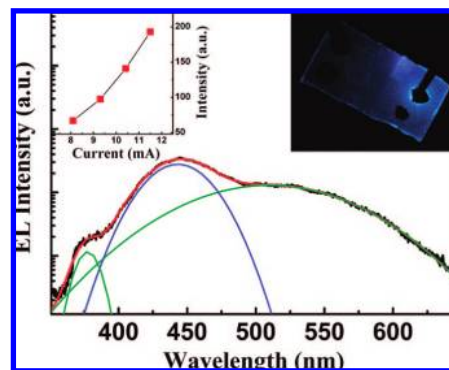


Figure 3. Room-temperature EL spectrum of the $n\text{-Mg}_{0.12}\text{Zn}_{0.88}\text{O}$ – MgO – $p\text{-GaN}$ heterojunction diode at a forward injection current of 11.5 mA. EL intensity of the 374 nm peak as a function of the injection current is shown in the left inset, and the right inset shows a typical emission photograph of the heterojunction diode.

at around 530 nm in the spectrum, which is a typical deep-level-related emission in ZnO-based materials. The PL spectrum of the GaN layer is dominated by a broad peak at about 430 nm, which is frequently observed in Mg-doped $p\text{-GaN}$ and can be attributed to the transition between deep donors and Mg-related acceptors.¹⁹ The fringes, just as those observed in the spectrum of $\text{Mg}_{0.12}\text{Zn}_{0.88}\text{O}$, are resulted from interference.

The current–voltage (I – V) curve of the $n\text{-Mg}_{0.12}\text{Zn}_{0.88}\text{O}$ – MgO – $p\text{-GaN}$ diode structure is illustrated in Figure 2. Obvious rectifying behaviors with a turn-on voltage of about 8 V are observed in the I – V curve. Shown in the inset of Figure 2 is the I – V curve of the Ni–Au electrode on $p\text{-GaN}$ and the In electrode on $n\text{-Mg}_{0.12}\text{Zn}_{0.88}\text{O}$. The linear I – V curves reveal that ohmic contacts have been obtained in both cases.

The EL spectrum of the heterojunction diode with the injection of continuous current is shown in Figure 3. The EL spectrum can be well-fitted by three Gaussian peaks centered at about 374, 440, and 520 nm. We note that the sharp cutoff on the short-wavelength side of the 374 nm emission is a result of self-absorption of the MgZnO layer. By comparing the EL spectrum with the PL spectrum, one can conclude that the peaks at 374 and 520 nm come from the $\text{Mg}_{0.12}\text{Zn}_{0.88}\text{O}$ layer, while the peak at 440 nm comes from the GaN layer. The variation in EL intensities for the peak at 374 nm on the injection current is shown in the left inset of Figure 3. It is observed that the EL intensity increases almost linearly with increasing current injection in the investigated range. A photograph of the

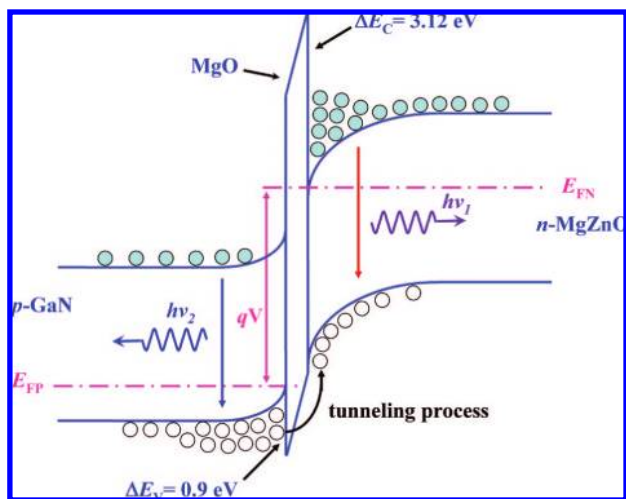


Figure 4. Schematic of band alignments of the $n\text{-Mg}_{0.12}\text{Zn}_{0.88}\text{O}$ – MgO – $p\text{-GaN}$ heterojunction under forward bias.

heterojunction diode is shown in the right inset of Figure 3, in which the black spots are electrodes. Clear emission from the entire junction area can be observed from the photograph. Note that the 374 nm peak is the second shortest wavelength for EL emissions ever observed in ZnO-based pn junctions to the best of our knowledge; only the 363 nm peak reported for a ZnBeO pn homojunction is shorter.²⁰ However, because reliable and stable p -doping of ZnO is difficult, a pn junction with a large band gap is not expected by most researchers when using ZnBeO . Additionally, the biotoxicity of beryllium impairs the usefulness of this material system.

The mechanism for the EL emissions can be well understood in terms of the carrier transportation process in the heterojunction. Considering that the electron affinity of ZnO, MgO, and GaN is 4.35,²¹ 0.80,²² and 4.20 eV,²³ respectively, the electron affinity of $\text{Mg}_{0.12}\text{Zn}_{0.88}\text{O}$ obtained by linear fitting of ZnO and MgO is about 3.92 eV. The conduction band offsets (CBO) at the $\text{Mg}_{0.12}\text{Zn}_{0.88}\text{O}$ – MgO interface and the GaN– MgO interface are 3.12 and 3.40 eV, respectively, and the corresponding valence band offsets (VBO) at the two interfaces are 1.02 and 0.90 eV, respectively. A schematic of the band alignments in the heterojunction under forward bias is shown in Figure 4. The role of the MgO layer in affecting the carrier transportation process is very similar to that in the $n\text{-ZnO}$ – $p\text{-GaN}$ heterojunction.¹¹ Briefly, because of the large CBO between MgZnO and MgO (3.12 eV), most electrons will be confined in the MgZnO layer under forward bias. The situations for holes are different. The VBO between GaN and MgO is relatively small (1.02 eV), and the band of MgO will bend significantly because of the bias applied. The band bending of MgO will reduce the effective barrier height at the GaN–MgO interface, considering the small thickness of the MgO layer. Consequently, holes can tunnel through the MgO dielectric layer and enter into the MgZnO layer. The reason why the emission from GaN is also observed in our experiment may be because of the fact that the thickness of the MgO layer is very small (20 nm), and some electrons can also tunnel through the MgO layer and enter into the GaN layer from the $n\text{-MgZnO}$ layer. It is rational to speculate that via proper adjustment of the thickness of the MgO layer, the emission from the GaN layer can be suppressed and that from the MgZnO layer can be greatly enhanced.

Conclusions

In conclusion, $\text{Mg}_x\text{Zn}_{1-x}\text{O}$ -based heterojunction diodes have been fabricated by integrating $n\text{-Mg}_{0.12}\text{Zn}_{0.88}\text{O}$ and $p\text{-GaN}$ together employing an MgO dielectric layer as an electron-blocking barrier. Under forward bias, an EL emission at around 374 nm from the $\text{Mg}_{0.12}\text{Zn}_{0.88}\text{O}$ layer was observed at room temperature. This is one of the shortest EL wavelengths reported in ZnO-based pn junctions. One can safely suppose that by further expanding the band gap of the MgZnO layer, we can attain EL emissions with even shorter wavelengths. Therefore, the results reported in this paper may open a door for ZnO-based short-wavelength light-emitting devices.

Acknowledgment. This work is supported by the National Natural Sciences Foundation of China (NNSFC) Key Project (50532050), the 973 Program (2006CB604906 and 2008CB317105), the Knowledge Innovation Program of the Chinese Academy of Sciences (KJCX3.SYW.W01), and the NNSFC (10674133, 10774132, and 60776011).

References and Notes

- (1) Look, D. C.; Claflin, B.; Alivov, Ya. I.; Park, S. J. *Phys. Status Solidi A* **2004**, *201*, 2203.
- (2) Xi, Y. Y.; Hsu, Y. F.; Djurišić, A. B.; Ng, A. M. C.; Chan, W. K.; Tam, H. L.; Cheah, K. W. *Appl. Phys. Lett.* **2008**, *92*, 113505.
- (3) Park, W. I.; Yi, G. C. *Adv. Mater.* **2004**, *16*, 87.
- (4) Jiao, S. J.; Lu, Y. M.; Shen, D. Z.; Zhang, Z. Z.; Li, B. H.; Zhang, J. Y.; Yao, B.; Liu, Y. C.; Fan, X. W. *Phys. Status Solidi C* **2006**, *4*, 972.
- (5) Rogers, D. J.; Teherani, F. H.; Yasan, A.; Minder, K.; Kung, P.; Razeghi, M. *Appl. Phys. Lett.* **2006**, *88*, 141918.
- (6) Sun, J. W.; Lu, Y. M.; Liu, Y. C.; Shen, D. Z.; Zhang, Z. Z.; Li, B. H.; Zhang, J. Y.; Yao, B.; Zhao, D. X.; Fan, X. W. *J. Phys. D: Appl. Phys.* **2008**, *41*, 155103.
- (7) Dong, J. W.; Osinsky, A.; Hertog, B.; Dabiran, A. M.; Chow, P. P.; Heo, Y. W.; Norton, D. P.; Pearton, S. J. *J. Electron. Mater.* **2005**, *34*, 416.
- (8) Alivov, Ya. I.; Johnstone, D.; Özgür, Ü.; Avrutin, V.; Fan, Q.; Akarcar-Biyikli, S.; Morkoç, H. *Jpn. J. Appl. Phys., Part 1* **2005**, *44*, 7281.
- (9) Ohta, H.; Kawamura, K.; Orita, M.; Hirano, M.; Sarukura, N.; Hosono, H. *Appl. Phys. Lett.* **2000**, *77*, 475.
- (10) Alivov, Ya. I.; Van Nostrand, J. E.; Look, D. C.; Chukichev, M. V.; Ataev, B. M. *Appl. Phys. Lett.* **2003**, *83*, 2943.
- (11) Zhu, H.; Shan, C. X.; Yao, B.; Li, B. H.; Zhang, J. Y.; Zhang, Z. Z.; Zhao, D. X.; Shen, D. Z.; Fan, X. W.; Lu, Y. M.; Tang, Z. K. *Adv. Mater.*, DOI: 10.1002/adma.200802907.
- (12) Ohtomo, A.; Kawasaki, M.; Koida, T.; Masubuchi, K.; Koinuma, H.; Sakurai, Y.; Yoshida, Y.; Yasuda, T.; Segawa, Y. *Appl. Phys. Lett.* **1998**, *72*, 2466.
- (13) Sharma, A. K.; Nerayan, J.; Muth, J. F.; Teng, C. W.; Jin, C.; Kvit, A.; Kolbas, R. M.; Holland, O. W. *Appl. Phys. Lett.* **1999**, *75*, 3327.
- (14) Ohtomo, A.; Shiroki, R.; Ohkubo, I.; Koinuma, H.; Kawasaki, M. *Appl. Phys. Lett.* **1999**, *75*, 4088.
- (15) Makino, T.; Tamura, K.; Chia, C. H.; Segawa, Y.; Kawasaki, M.; Ohtomo, A.; Koinuma, H. *Appl. Phys. Lett.* **2002**, *81*, 2172.
- (16) Matsui, H.; Tabata, H.; Hasuike, N.; Harima, H. *J. Appl. Phys.* **2006**, *99*, 024902.
- (17) Park, W. I.; Yi, G.-C.; Jang, H. M. *Appl. Phys. Lett.* **2001**, *79*, 2022.
- (18) Dong, X.; Zhang, B. L.; Li, X. P.; Zhao, W.; Xia, X. C.; Zhu, H. C.; Du, G. T. *J. Phys. D: Appl. Phys.* **2007**, *40*, 7298.
- (19) Kaufmann, U.; Schlotter, P.; Obloh, H.; Kohler, K.; Maier, M. *Phys. Rev. B* **2000**, *62*, 10867.
- (20) Ryu, Y. R.; Lee, T. S.; Lubguban, J. A.; White, H. W.; Kim, B. J.; Park, Y. S.; Youn, C. J. *Appl. Phys. Lett.* **2006**, *88*, 241108.
- (21) Aranovich, J. A.; Golmayo, D. G.; Fahrenbruch, A. L.; Bube, R. H. *J. Appl. Phys.* **1980**, *51*, 4260.
- (22) Yamashita, J. *Phys. Rev.* **1958**, *111*, 733.
- (23) Qiao, D.; Yu, L. S.; Lau, S. S.; Redwing, J. M.; Lin, J. Y.; Jiang, H. X. *J. Appl. Phys.* **2000**, *87*, 801.